IBEC
Institute for Bioengineering of Catalonia

SHAPING THE PRESENT AND FUTURE OF MEDICINE WITH BIOENGINEERING

Urease-powered nanomotors for enhancing bladder cancer chemotherapy

Kristin Fichna[1,2], *Maria Crespo-Cuadrado*[1], *Acsah Konuparamban*[3], *Maria Crespo-Cuadrado*[1], *Valerio Di Carlo*[1], *David Esporrín-Ubieto*[1], *Ines Macías Tarrío*[1], *Shuqin Chen*[1], *María Gómez-Martínez*[3], *Anna C. Bakenecker*[1], *Antoni Vilaseca*[4], *Jordi Llop*[3], *Samuel Sánchez Ordóñez*[1,5]

[1]Institute for Bioengineering of Catalonia (IBEC), The Barcelona Institute for Science and Technology (BIST), Baldiri i Reixac 10-12, 08028 Barcelona, Spain
[2]Doctorate in Biotechnology, Facultat de Farmàcia i Ciències de l'Alimentació, Universitat de Barcelona, Avda. Diagonal 643, 08028 Barcelona, Universitat de Barcelona, Spain
[3]CIC biomaGUNE, Basque Research and Technology Alliance (BRTA), Paseo Miramón 182, 20014, Donostia/San Sebastián, Spain
[4]Uro-Oncology Unit, Hospital Clinic, University of Barcelona, Spain
[5]Institució Catalana de Recerca I Estudis Avancats (ICREA), 08010 Barcelona, Spain

Motivation and Aim

- Bladder cancer is 9th most common cancer worldwide and one of the most expensive ones to treat
- Current therapies prolong patient survival, but are characterized by high relapse rates

➢ Urgent need to improve existing therapies

- Equipping nanoparticles with ability to move (=nanomotors) might help to improve the delivery efficiency of clinically used chemotherapeutics[1]
- Urease-powered nanomotors can move in presence of urea, which is component of urine, and accumulate in bladder tumors[2,3,4]

➢ Using urease-nanomotors based on mesoporous silica nanoparticles (MSNP) loaded with Mitomycin C, the gold standard of care in intravesical bladder cancer chemotherapy, might be able to improve the therapeutic efficiency the drug

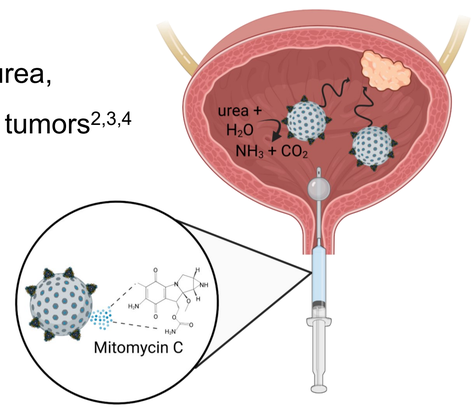

Nanoparticle Characterization and drug loading

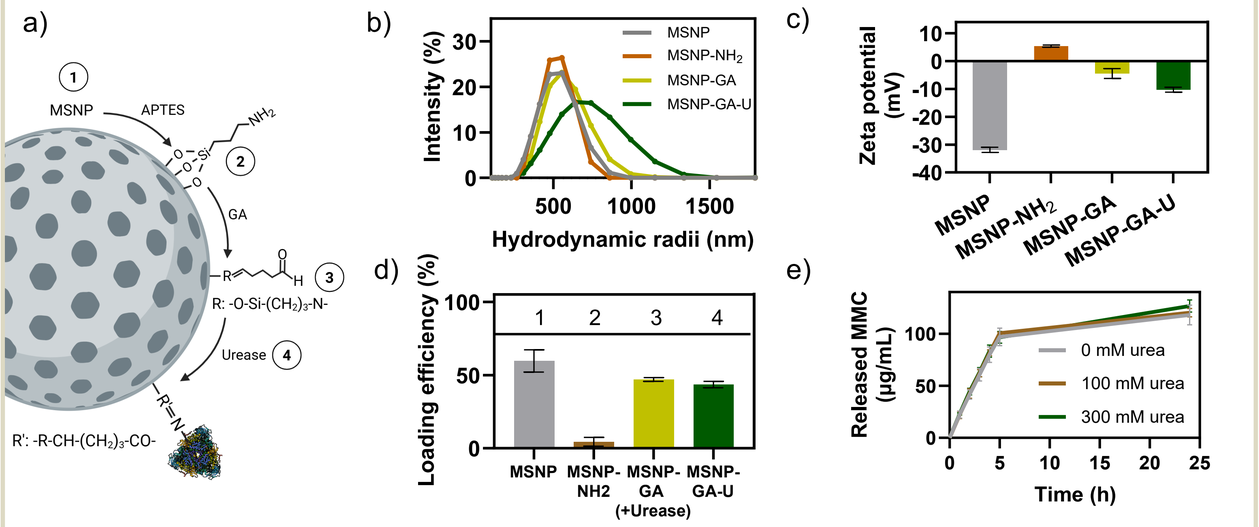

Figure 1: Synthesis and Characterization of Urease-Nanomotors. a) Schematic illustration of surface modification of MSNP to obtain Urease-Nanomotors. b) Hydrodynamic radii (nm) of particles in each functionalization step. c) Surface charge evolution during surface modification of MSNP to obtain urease-NM. d) Drug-loading efficiency of MMC at different steps of the functionalization of MSNP as indicated in the schematics. e) Time- dependent cumulative release (µg/mL) of MMC from NM in presence of different concentrations of urea (n=3).

Active motion of Nanomotors@MMC

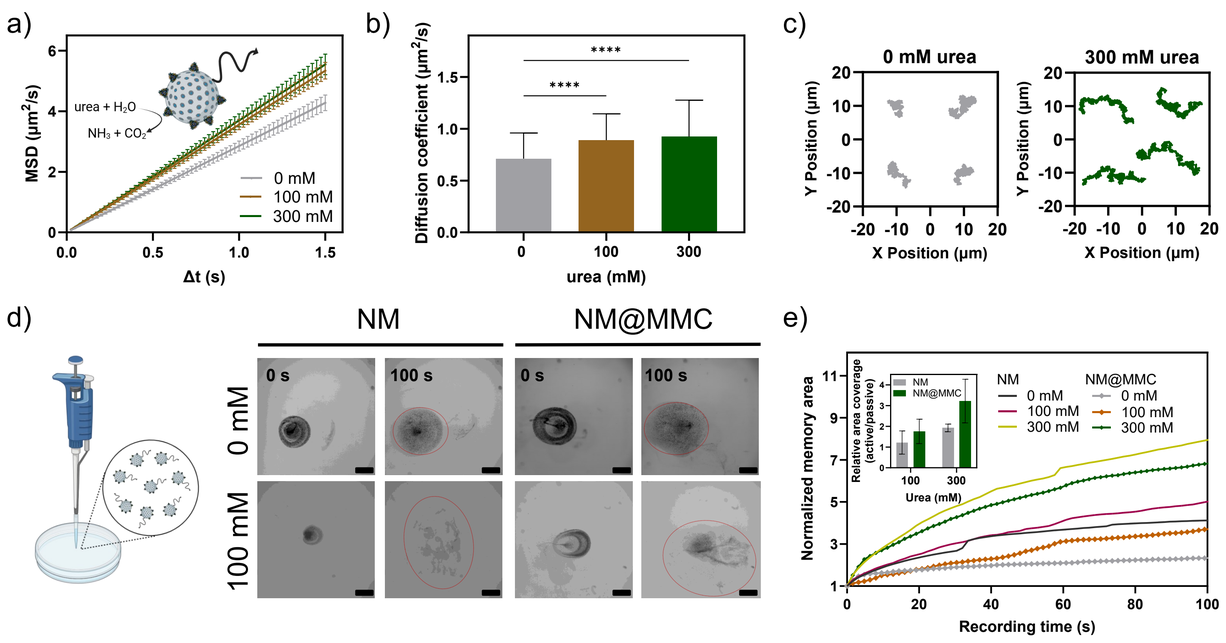

Figure 2: Single particle-and collective motion analysis of NM and NM@MMC. a) Mean Square Displacement (±SE) of NM@MMC in PBS at 0-, 100-and 300 mM of urea. b) Diffusion coefficient of NM@MMC obtained by optical tracking at different concentrations of urea (n>100 ± SE), Statistical significance (one-way ANOVA) is indicated when appropriate (*p < 0.05, **p < 0.01, ***p < 0.001, ****p < 0.0001). c.) Representative tracking trajectories of NM@MMC during 30 s in 0- and 300 mM of urea. d) Video snapshots of collective motion of nanomotors taken from the top-view. The scalebar corresponds to 1 mm. c) Area covered by NM swarms normalized to the initial area (t=0 s) as a function of time. Inlet: relative covered area of NM swarms at t=100 s. The relative covered area was calculated by normalizing the area covered by NM and NM@MMC in 100 mM and 300 mM urea (t=100 s) with the area covered by NM and NM@MMC in 0 mM urea (t=100s).

In vivo tumor growth inhibition and recurrence prevention

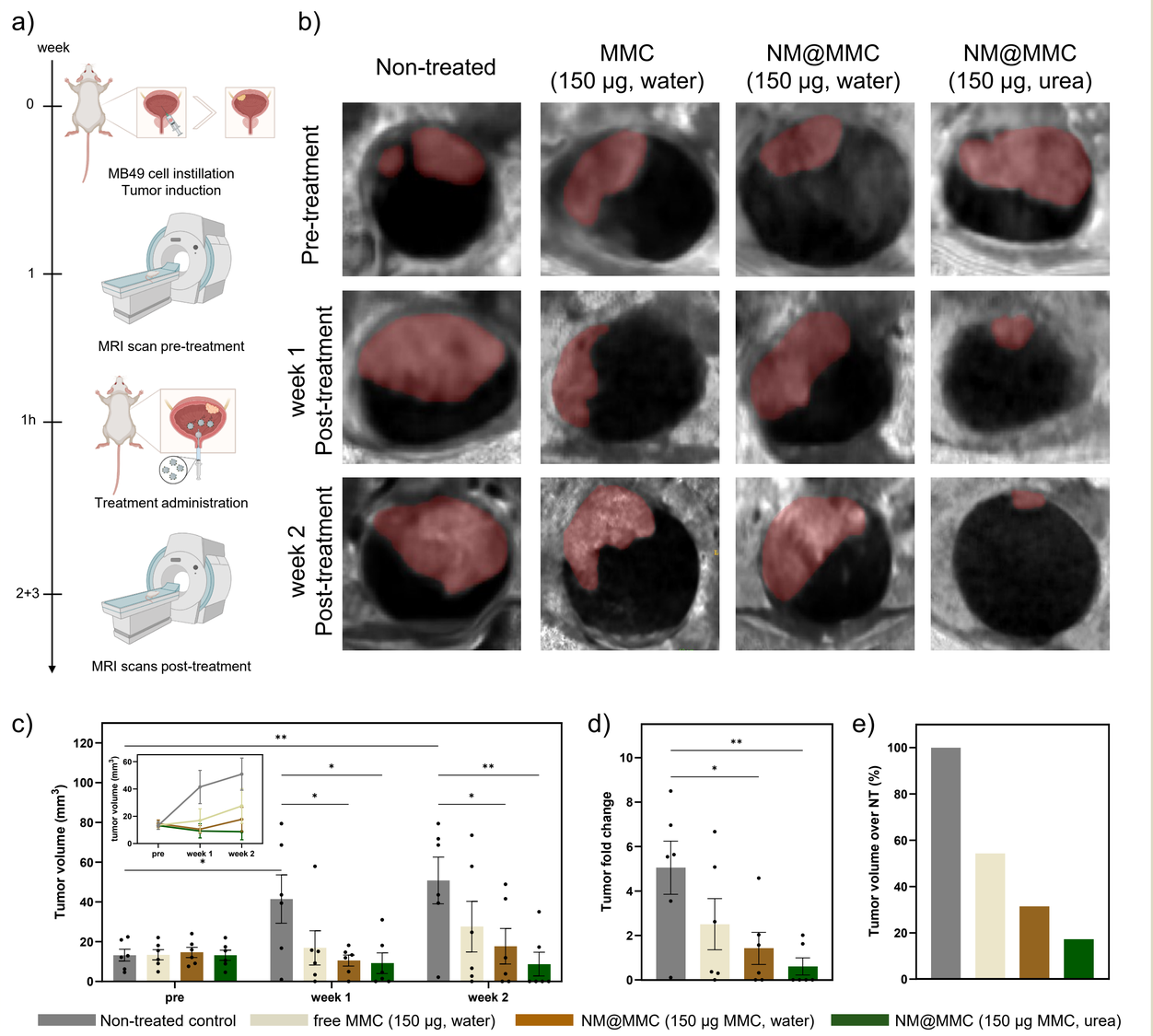

Figure 4: Therapeutic effect of MMC-loaded urease-Nanomotors in an orthotopic murine bladder cancer model. a.) Schematic illustration of timeline of intravesical chemotherapy using drug-loaded NM. b.) Representative 2D DW-MRI images of the bladder (hypointense circular region) of representative mice before and after treatment. c.) Tumor volumes as determined using MRI before and after treatment. Results are expressed as bar diagrams (mean ± SE; one dot per animal). Inlet: Average tumor volume evolution over time. d.) Tumor fold change for 2-weeks post-treatment. Results are expressed as bar diagrams (mean ± SE; one dot per animal). e) Tumor volumes normalized over control condition (non-treated group) for 2 weeks post-treatment. Statistical analysis for tumor volumes was performed via two-way ANOVA followed by Tukey's multiple comparison test. Statistical analysis for tumour fold change was performed via one-way ANOVA followed by Tukey's multiple comparison test. Statistical significance is indicated when appropriate (*p < 0.05, **p < 0.01, ***p < 0.001, ****p < 0.0001).

In vitro toxicity

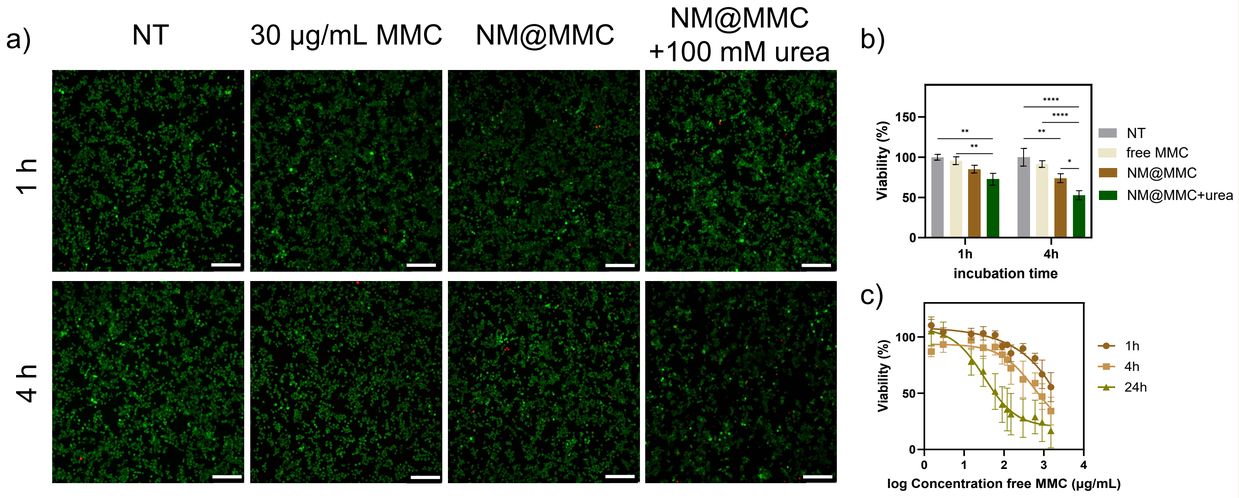

Figure 3: Therapeutic effect of MMC-loaded Urease-NM to MB49 cells. a) LIVE/DEAD images of non-treated cells and cells treated with free MMC (30 µg/mL, corresponds to amount of loaded MMC-formulation in 5 µg/mL of NM), NM@MMC at 5 µg/mL in and NM@MMC in presence of 100 mM of urea. Images were taken after 1 h and 4 h of incubation. The scale bar corresponds to 200 µm b.) Quantification of viable cells based on LIVE/DEAD imaging (n=3). c.) Representation of non-linear regression of the IC50 for MMC in MB49 cells after 1h, 4h and 24h of incubation. The results are represented as mean ± SD for (n = 3 biological replicates). Statistical significance (two-way ANOVA) is indicated when appropriate (*p < 0.05, **p < 0.01, ***p < 0.001, ****p < 0.0001).

Conclusion

Urease-powered nanomotors were successfully synthesized and characterized. Nanomotors@MMC are *in vitro* almost 20x more efficient than free Mitomycin C. *In vivo*, these nanomotors outperform the free drug in terms of tumor growth inhibition and recurrence prevention. Thus, this technology might be able to tackle major challenges in bladder cancer chemotherapy.

Acknowledgement

The research leading to this results has received funding from the European Research Council (ERC) under the European Union's Horizon 2020 research and innovation programme (Grant 866348, i-NANOSWARMS) as well as from "la Caixa" Foundation under the grant agreement LCF/PR/HR20/52400004 (Bladdebots). Additionally, special thanks goes to Oriol Jutglar Soler who helped with the evaluation of the single particle motion. The illustrations were created with biorender.com

References

(1) Hortelão, A. C.; Patiño, T.; Perez-Jiménez, A.; Blanco, À.; Sánchez, S. ***Adv. Funct. Mater.*** **2018**, *28* (25), 1–10.
(2) Hortelao, A. C.; Simó, C.; Guix, M.; Guallar-Garrido, S.; Julián, E.; Vilela, D.; Rejc, L.; Ramos-Cabrer, P.; Cossío, U.; Gómez-Vallejo, V.; Patiño, T.; Llop, J.; Sánchez, S. ***Sci. Robot.*** **2021**, *6* (52), eabd2823.
(3) Simó, C.; Serra-Casablancas, M.; Hortelao, A. C.; Di Carlo, V.; Guallar-Garrido, S.; Plaza-García, S.; Rabanal, R. M.; Ramos-Cabrer, P.; Yagüe, B.; Aguado, L.; Bardia, L.; Tosi, S.; Gómez-Vallejo, V.; Martín, A.; Patiño, T.; Julián, E.; Colombelli, J.; Llop, J.; Sánchez, S. ***Nat. Nanotechnol.*** **2024**.

Generalitat de Catalunya · Universitat de Barcelona · Universitat Politècnica de Catalunya BarcelonaTech · CERCA Centres de Recerca de Catalunya · Excelencia Severo Ochoa · bist